Electronic Supplementary Material (ESI) for Green Chemistry.

Supporting Information

1,2,3 – Trimethoxypropane: a bio-sourced glyme as electrolyte for Lithium-O_2 batteries

Marta Alvarez-Tirado,[a] Laurent Castro,*[b] Shuai Qian,[c] Jason E. Bara,[c] Marco Di Gennaro,[d] Konstantinos Gkagkas,[b] Aurélie Guéguen,[b] and David Mecerreyes* [a,e]

[a] *POLYMAT University of the Basque Country UPV/EHU, Avenida Tolosa 72, Donostia-San Sebastian 2008, Spain*

[b] *Material Engineering Division, Toyota Motor Europe NV/SA, Technical Center, 1930 Zaventem, Belgium*

[c] *Department of Chemical & Biological Engineering, University of Alabama, Box 870203, Tuscaloosa, Alabama 35487-0203, United States*

[d] *Nanomat, Q-Mat, CESAM, European Theoretical Spectroscopy Facility, Universite de Liege, B-4000 Liege, Belgium*

[e] *Ikerbasque, Basque Foundation for Science, E-48011, Bilbao, Spain*

AUTHOR INFORMATION

*e-mail: david.mecerreyes@ehu.es, Laurent.Castro@toyota-europe.com

EXPERIMENTAL DETAILS

Synthesis of 1,2,3-Trimethoxypropane (TMP)[1]

To a 250 mL pressure vessel loaded with NaOH (40.0 g, 1.0 mol) and dimethyl sulfoxide (80 mL) was added 1,3-dimethoxypropane-2-ol (60.1 g, 0.5 mol). The mixture was stirred at RT for 30 min, followed by a singular addition of methyl iodide (142.0 g, 2 equiv.). The temperature was raised to 50 °C and the reaction was allowed to run for 6 h before cooling down to RT. Solids were filtered and washed with 50 mL Et_2O. The liquid mixture was dissolved into 500 mL Et_2O, washed in sequence with 2×60 mL DI water and 3×80 mL saturated $NaHCO_3$ solution, and dried over anhydrous $MgSO_4$. The solids were then filtered and solvent was removed by rotary evaporation under reduced pressure. The remaining liquid was distilled to afford 34.7 g (51.7%) 1,2,3-TMP. ^{1}H NMR (360 MHz, DMSO-d_6) δ 3.46 – 3.34 (m, 5H), 3.33 (s, 3H), 3.24 (d, J = 2.4 Hz, 6H). ^{1}H NMR data (Fig. S7) agreed well with that in literature[1].

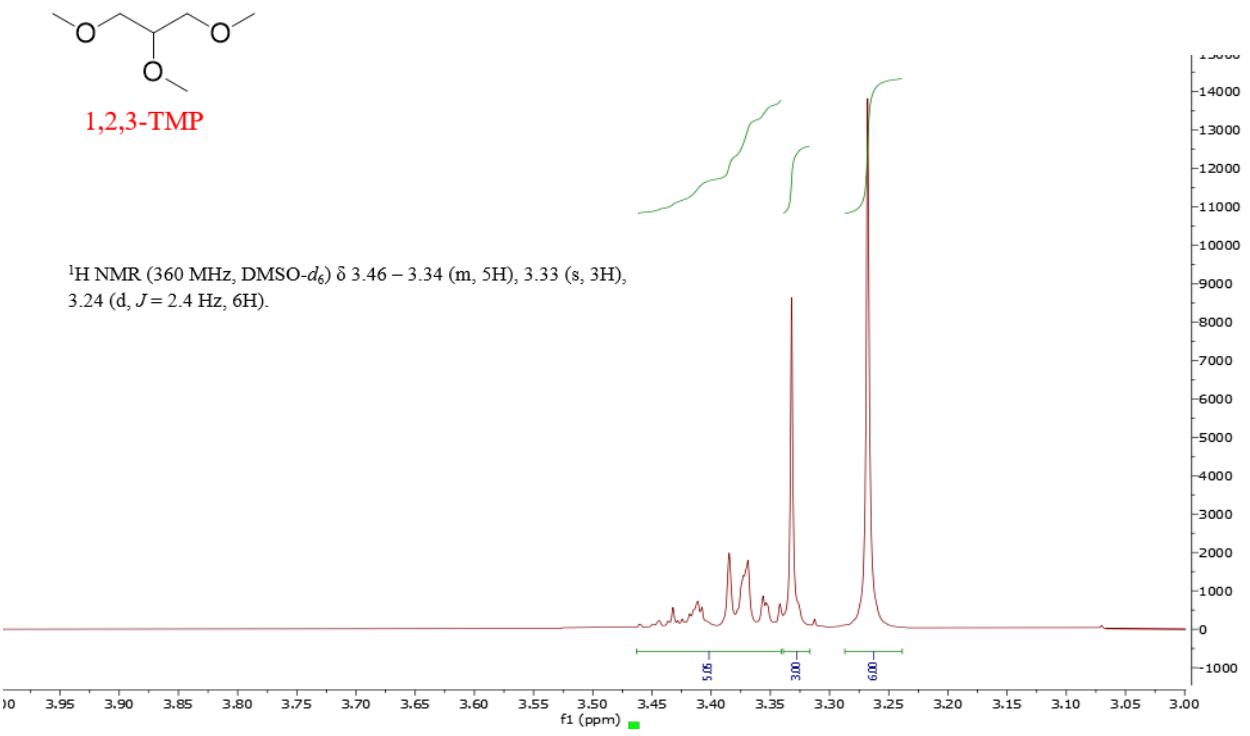

Fig. S1. ^{1}H NMR spectra of 1,2,3-TMP.

Simulation Details

All-atom Molecular Dynamics (MD) simulations were performed on two systems: LiTFSI salt diluted in diglyme solvent (Liquid-G2) and 1,2,3 – TMP solvent (Liquid-TMP). The CLANDP force field[2–6] was used. The ratio between the number of solvent molecules and the number of salt molecules was fixed to 7 in order to respect the experimental value. The number of anions was fixed to 50, for a total of 400 molecules in the simulation box. Periodic boundary conditions were used.

The initial configuration of the box was realized with PACKMOL[6], while the MD simulation were performed within the GROMACS simulation package version 2021.2 [7–13].

The system composed by solvent and anion was then neutralized. An energy minimization was performed with a 50k steps and a tolerance of 10 kJ mol^{-1} nm^{-1}, followed by a canonical NVT equilibration of 2 ns (1M steps of 2fs each). Coordinates were saved each 100 steps. The coulomb and van der Waals cutoff for intermolecular interactions were set to 1.0 nm each. Long-range electrostatic interactions were treated by means of the Particle-mesh Ewald method with cubic (i.e. 4^{th} order polynomial) interpolation method and 0.16 spacing in the Fourier space. A leap-frog integrator (md) was employed to integrate Newton's equations, with a Verlet cutoff-scheme within an update of the neighbor list each 10 steps for neighbor search. H-bonds were constrained with the LINCS algorithm (we used the default values of 1 iteration number and 4 for the order in the expansion of the constraint coupling matrix). The temperature bath is controlled through an independent thermostat for each residue (DIG/TMP, TFS and LI), with a temperature coupling using velocity rescaling with a stochastic term[14] and a temperature reference of 1 K.

A further isothermal-isobaric NPT equilibration was performed for another 2 ns (1M steps of 2 fs), reading the velocities from the previous step. A Berendsen barostat was imposed, with a reference pressure of 1atm and an isotropic pressure coupling of 1 bar and time constant of 1 ps. To insure statistical independence, a second NPT equilibration run was performed with 10 ns (10M steps of 1 fs) and similar barostat/thermostat characteristics. Water compressibility of $4.5e^{-5}$ bar^{-1} was used.

Finally, five independents MD production runs were initiated reading velocities from this last run, and the results here presented are averaged on top of them.

Electrolyte components properties

Table S1 Key properties of most common ether based molecules, including 1,2,3 - TMP.

Solvent	Empirical formula	bp (°C)	mp (°C)	Flash point (°C)	Autoignition temperature (°C)	Density, 25 °C (g/cm3)	Dielectric constant[15], 25 °C	Safety pictograms and danger health hazards*
Monoglyme (DME, G1)	$C_4H_{10}O_2$	85	-141	-2	202	0.867	6.99	 H315 – Skin irritation. H332 – Harmful if inhaled. H360FD - May damage fertility or the unborn child.
Diglyme (G2)	$C_6H_{14}O_3$	162	-64	57	188	0.944	7.23	 H360FD - May damage fertility or the unborn child.
Triglyme (G3)	$C_8H_{18}O_4$	216	-45	111	190	0.986	7.51	 H319 – Serious eye irritation. H360Df - May damage the unborn child. Suspected of damaging fertility.
Tetraglyme (TEGDME, G4)	$C_{10}H_{22}O_5$	275	-30	141	265	1.009	7.68	

Solvent	Empirical formula	bp (°C)	mp (°C)	Flash point (°C)	Autoignition temperature (°C)	Density, 25 °C (g/cm3)	Dielectric constant[15], 25 °C	Safety pictograms and danger health hazards*
								H319 – Serious eye irritation. H360Df - May damage fertility or the unborn child.
1,2,3 TMP	$C_6H_{14}O_3$	148	-	45.5***	Unknown	0.942	Unknown	***According to OECD guidelines and source: ✓ Low acute toxicity ✓ No skin sensitization ✓ No mutagenicity ✓ No ecotoxicity in aquatic environment ▪ It is eye irritant. Major hazards have not been determined yet.
1,3 – Dioxolane (DOL)	$C_3H_6O_2$	76	-95	-3	274	1.06	7.13	 H319 – Serious eye irritation. H360Df - May damage the unborn child. Suspected of damaging fertility.
1,3,5, - Trioxane (TRI)	$C_3H_6O_3$	114	64	45	410	1.38	15.55 **	

Solvent	Empirical formula	bp (°C)	mp (°C)	Flash point (°C)	Autoignition temperature (°C)	Density, 25 °C (g/cm3)	Dielectric constant[15], 25 °C	Safety pictograms and danger health hazards*
								H335 – May cause respiratory irritation. H361 – Suspected of damaging fertility or the unborn child.
Paraldehyde (PAR)	$C_6H_{12}O_3$	124	12	36	238	0.99	14.7	

*Data taken from source: Merck/Sigma-Aldrich safety data sheets. Only included health hazard codes in the text. Pictograms and associated hazards codes:

GHS02 – Flammable gases, aerosols, liquids or solids. Self-reactive substances and mixtures, pyrophoric liquids or solids, self-heating substances and mixtures, substances and mixtures that in contact with water emit flammable gases; or organic peroxides

GHS07 – Acute toxicity, skin irritation, eye irritation, skin sensitization or specific target organ toxicity.

GHS08 – Health hazard such as respiratory sensitization, germ cell mutagenicity, carcinogenicity, reproductive toxicity or specific target organ toxicity.

**At 65 °C

***Data taken from source: M. Sutter *et al., Green Chemistry*, 2013, **11**, 3020-3026, DOI : 10.1039/c3gc41082j

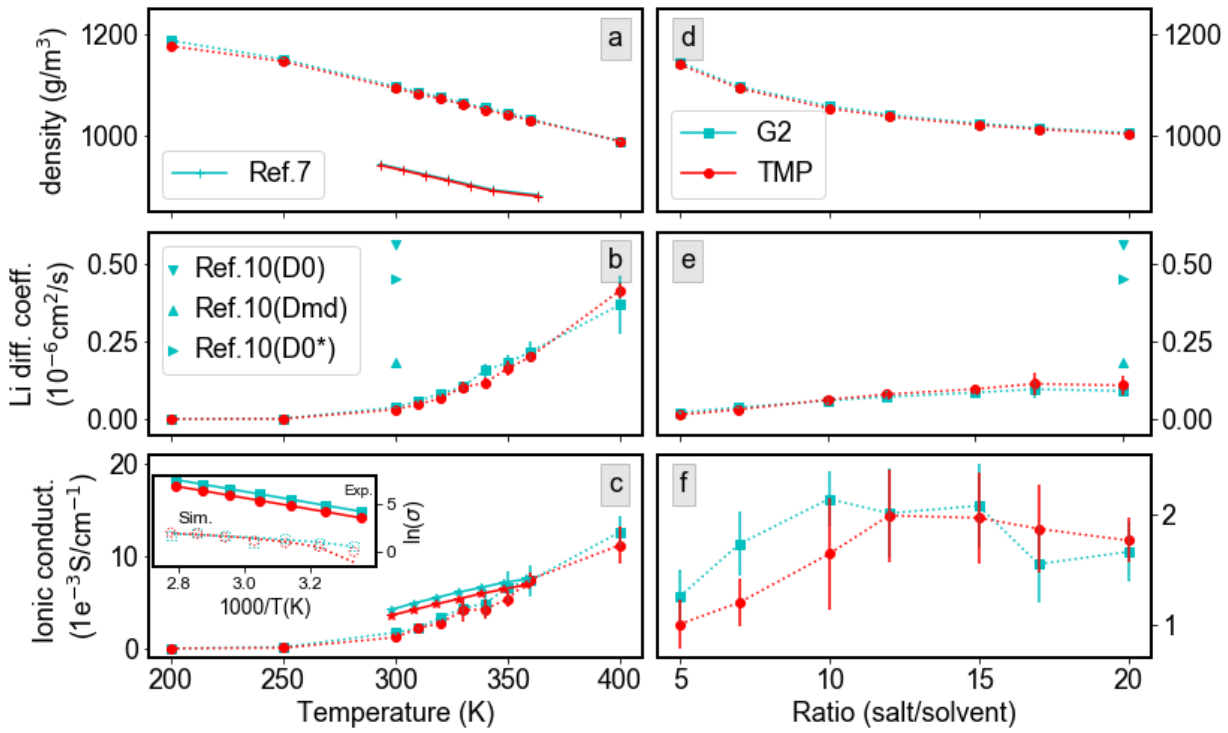

Fig. S2. Simulation results of Density (top panels, *a and d*)), Lithium diffusion coefficient (middle panel, *b and e*) and Lithium ionic conductivity (bottom panel, *c and f*); for increasing temperature (left column) and salt/solvent ratio (right column). Results are shown for diglyme-based electrolyte (*light blue*) and TMP-based electrolytes (*red*). Values from literature correspond as follows: Ref.7 (Flowers et. al)[1] and Ref.10.(Horwitz et al)[16].

Table S2. Fit values for the Arrhenius equation for both experimental methods and MD simulation.

Electrolyte [a]	Method	Fit	R^2
Liquid-G2	MD simulation	0.771	0.606
Liquid-G2	Experimental	0.512	0.999
Liquid-TMP	MD simulation	0.489	0.937
Liquid-TMP	Experimental	0.512	0.998

[a] 1M LiTFSI in the selected solvent.

Table S3. Compositions of GPE-based electrolytes in weight percentages.

Sample	Liquid electrolyte (1 M LiTFSI in xy[a])	TA[b]	DA[c]	PEGA[d]
GPE-xy50	50	5	5	40
GPE-xy70	70	5	5	20
GPE-xy80	80	5	5	10
GPE-xy90	90	5	5	0

[a] xy = selected ether based solvent.

[b] TA = glycerol propoxylate triacrylate

[c] DA = diethylene glycol diacrylate

[d] PEGA = poly(ethylene glycol) methyl ether acrylate

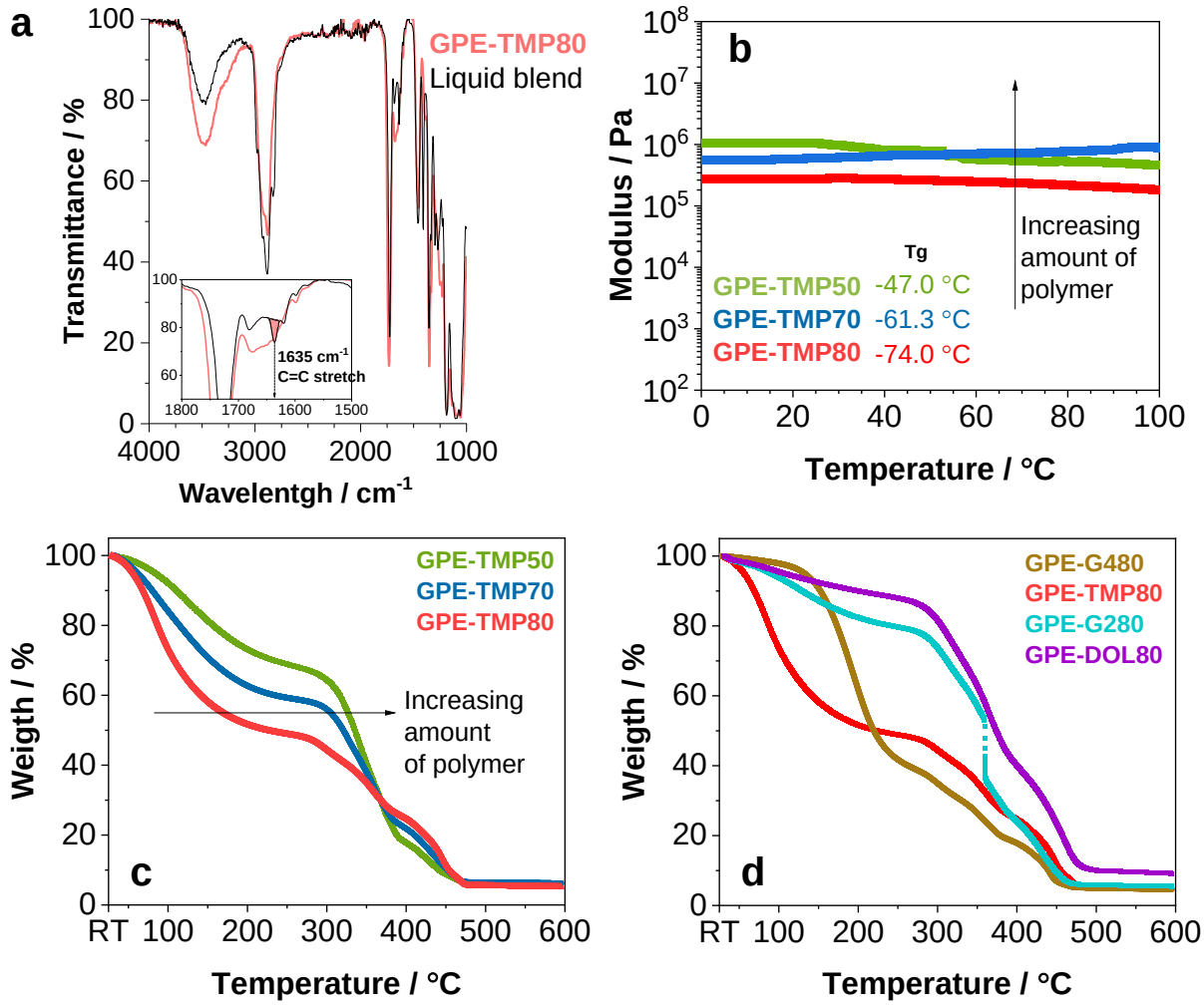

Fig. S3. a) FTIR spectra of GPE-TMP samples before (liquid blend) and after photopolymerisation. The 1635 cm-1 band, which is associated to the carbon double bond of acrylate functionalities, disappeared from the solid GPEs spectra; b) DMTA analysis at compression from 0 to 100 °C of TMP-based GPEs; and TGA analysis under nitrogen atmosphere at 10 °C/min of c) GPE-TMP based samples and d) GPEs made with the four plasticizers analyzed in this work.

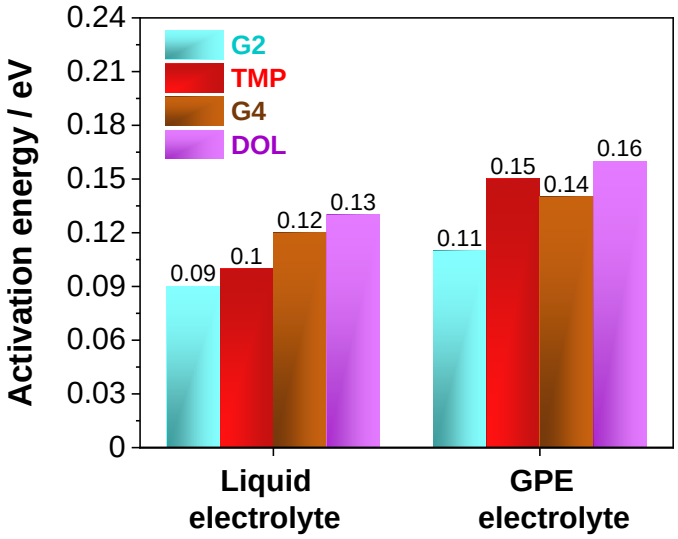

Fig. S4. Activation energies (eV) calculated following Arrhenius fittings of thermally-activated processes[17].

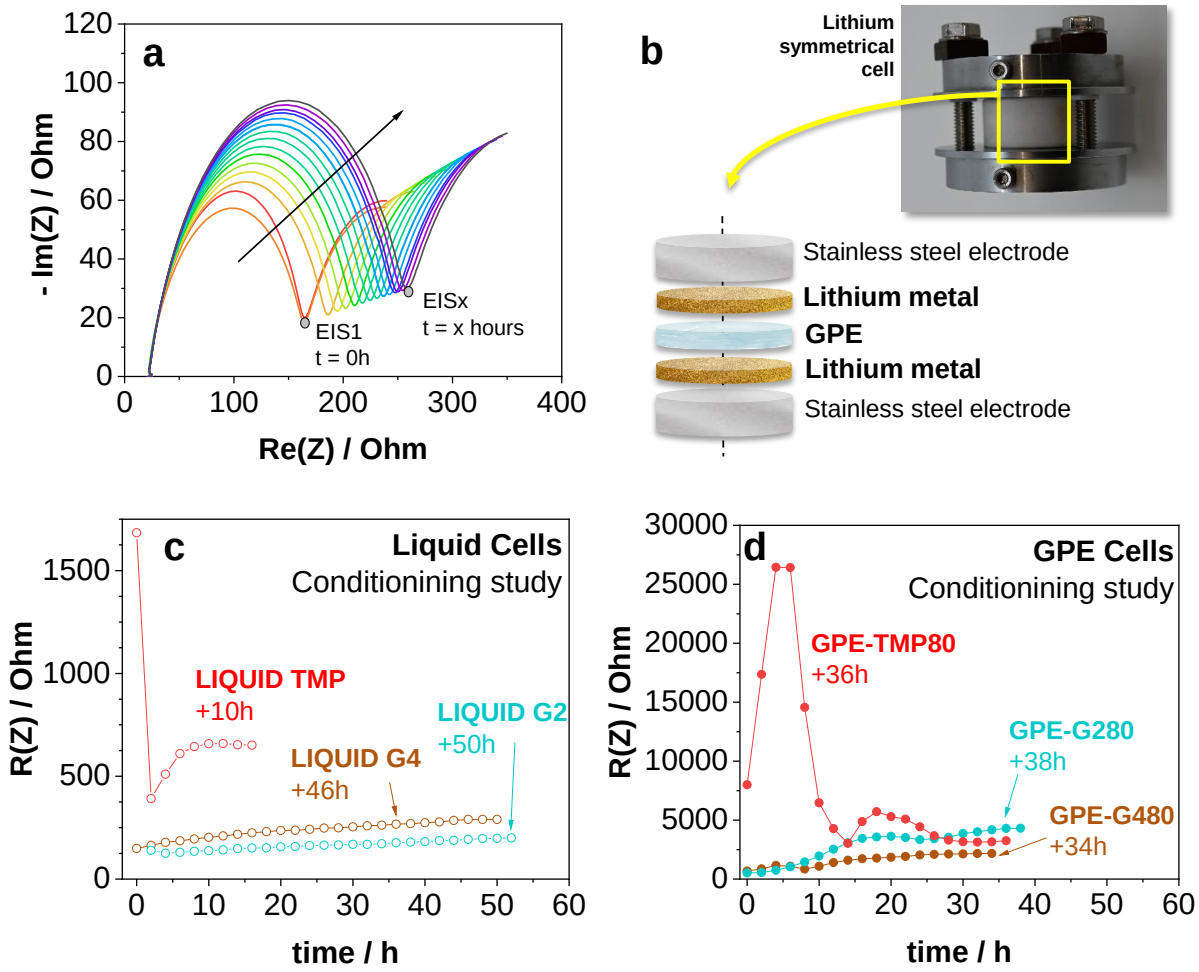

Fig. S5. a) Nyquist plots of lithium symmetrical cells using LIQ-G4 electrolyte showing the evolution of impedance at increasing timings; b) Scheme of lithium symmetric cell configuration used for conditioning time evaluation test; c) Evolution of impedance in time of cells using liquid electrolytes and d) Evolution of impedance in time of GPE-based cells. Please note that the scale used for the liquid and GPE cells are different.

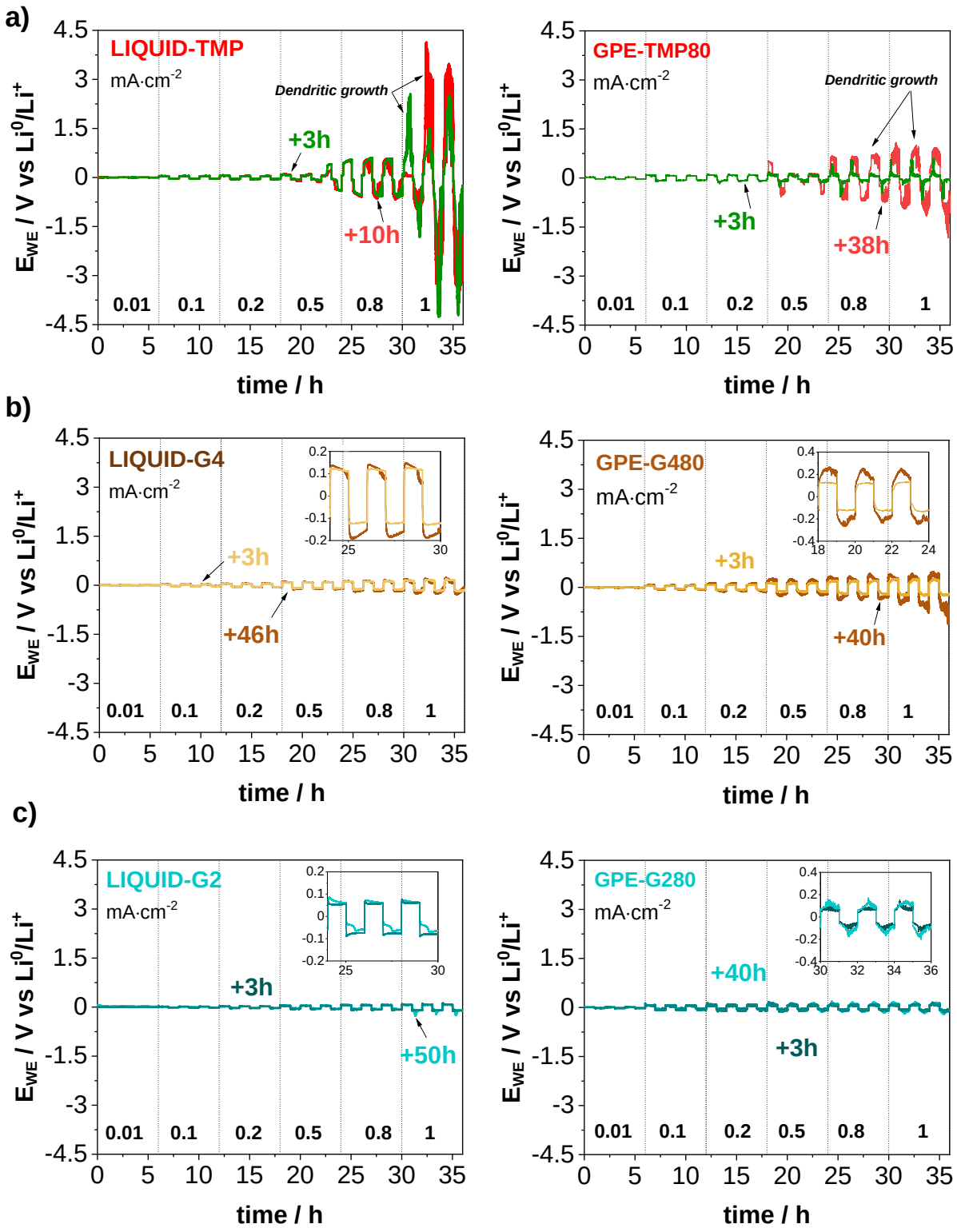

Fig. S6. Impact of conditioning time during lithium plating/striping cycles on symmetrical cells from 0.01 to 1 mAcm^{-2} using: a) LIQUID-TMT and GPE-TMP80 electrolytes; b) LIQUID-G4 and GPE-G480 electrolytes; and c) LIQUID-G2 and GPE-G280 electrolytes.

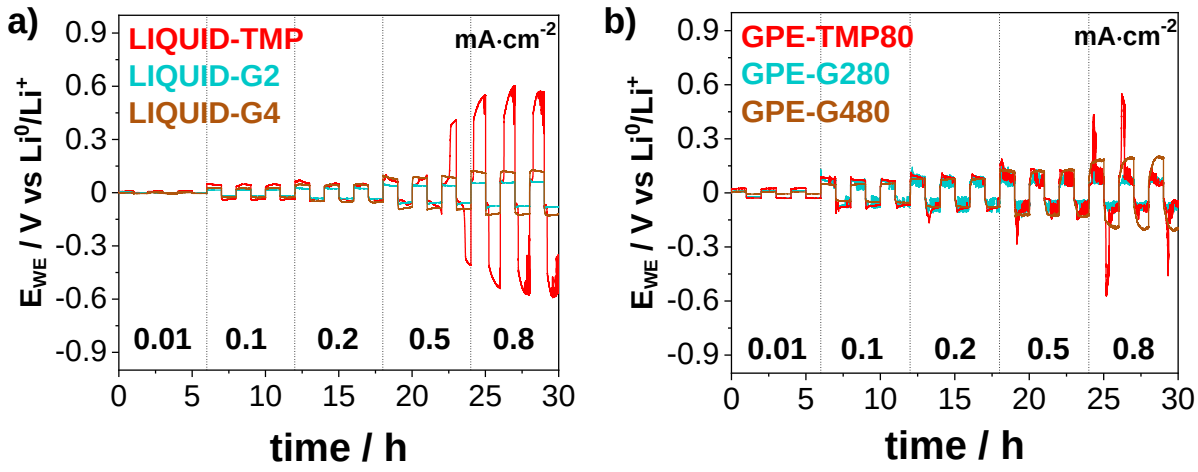

Fig. S7. Lithium stripping/platting curves at increasing current densities from 0.01 to 0.8 mA·cm^{-2} of cells using a) liquid electrolytes and b) gel polymer electrolytes.

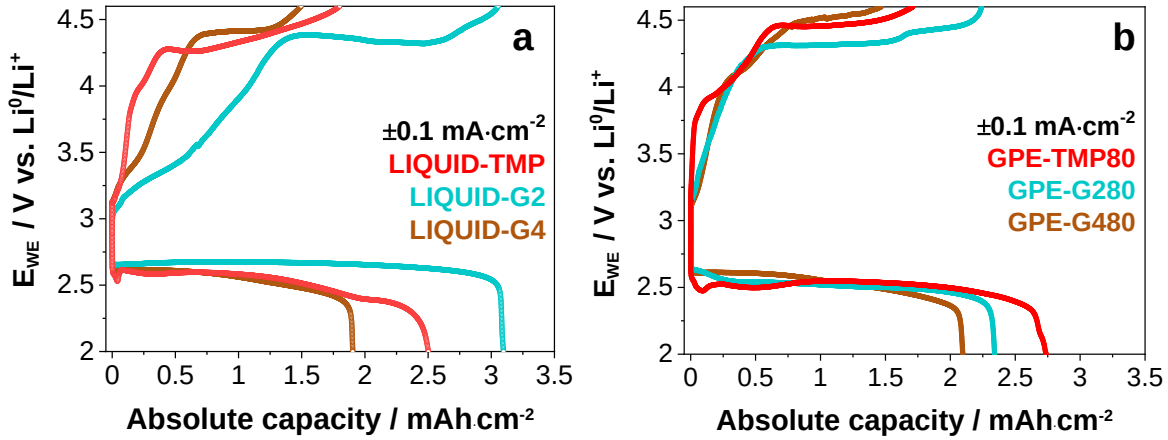

Fig. S8. Potential against absolute capacity during galvanostatic discharge/charge at ±0.1 mA·cm^{-2} and 25 °C (limiting potential of 4.3 V for charge and 2 V for discharge). First cycles in Li-O_2 cells of: a) Liquid electrolytes based on TMP, G2 and G4; b) GPE electrolytes with TMP, G2 and G4 plasticizers.

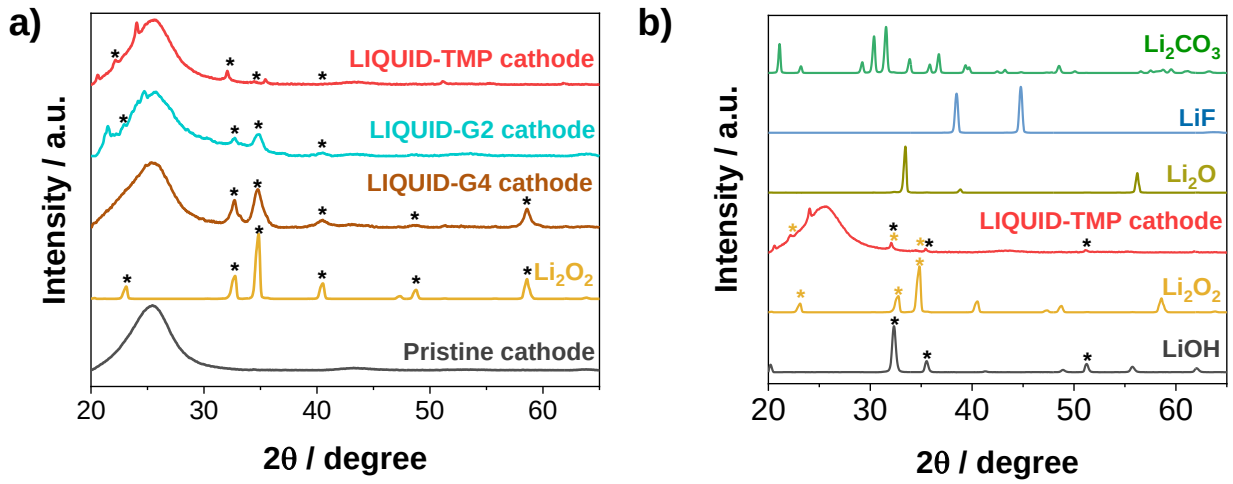

Fig. S9. X-ray diffraction (XRD) patterns of discharged cathodes of GPE Li-O_2 cells after first full discharge cycle: a) TMP, G2 and G4 samples compared with a pristine cathode and pure Li_2O_2 powder; and b) GPE-TMP80 discharged cathode pattern compared with different lithium compounds.

REFERENCES

1 B. S. Flowers, M. S. Mittenthal, A. H. Jenkins, D. A. Wallace, J. W. Whitley, G. P. Dennis, M. Wang, C. H. Turner, V. N. Emel'Yanenko, S. P. Verevkin and J. E. Bara, *ACS Sustain. Chem. Eng.*, 2017, **5**, 911–921.

2 J. N. C. Lopes and A. A. H. Pádua, *J. Phys. Chem. B*, 2004, **108**, 16893–16898.

3 J. N. Canongia Lopes, J. Deschamps and A. A. H. Pádua, *J. Phys. Chem. B*, 2004, **108**, 11250.

4 J. N. Canongia Lopes and A. A. H. Pádua, *J. Phys. Chem. B*, 2006, **110**, 19586–19592.

5 J. N. Canongia Lopes, A. A. H. Pádua and K. Shimizu, *J. Phys. Chem. B*, 2008, **112**, 5039–5046.

6 L. Martínez, R. Andrade, E. G. Birgin and J. M. Martínez, *J. Comput. Chem.*, 2009, **30**, 2157–2164.

7 H. J. C. Berendsen, D. van der Spoel and R. van Drunen, *Comput. Phys. Commun.*, 1995, **91**, 43–56.

8 E. Lindahl, B. Hess and D. van der Spoel, *J. Mol. Model.*, 2001, **7**, 306–317.

9 D. Van Der Spoel, E. Lindahl, B. Hess, G. Groenhof, A. E. Mark and H. J. C. Berendsen, *J. Comput. Chem.*, 2005, **26**, 1701–1718.

10 B. Hess, C. Kutzner, D. Van Der Spoel and E. Lindahl, *J. Chem. Theory Comput.*, 2008, **4**, 435–447.

11 S. Pronk, S. Páll, R. Schulz, P. Larsson, P. Bjelkmar, R. Apostolov, M. R. Shirts, J. C. Smith, P. M. Kasson, D. Van Der Spoel, B. Hess and E. Lindahl, *Bioinformatics*, 2013, **29**, 845–854.

12 S. Páll, M. J. Abraham, C. Kutzner, B. Hess and E. Lindahl, *Lect. Notes Comput. Sci. (including Subser. Lect. Notes Artif. Intell. Lect. Notes Bioinformatics)*, 2015, **8759**, 3–27.

13 M. J. Abraham, T. Murtola, R. Schulz, S. Páll, J. C. Smith, B. Hess and E. Lindah, *SoftwareX*, 2015, **1–2**, 19–25.

14 G. Bussi, D. Donadio and M. Parrinello, *J. Chem. Phys.*, , DOI:10.1063/1.2408420.

15 Landolt-Börnstein - Group IV Physical Chemistry, in *Static Dielectric Constants of Pure Liquids and Binary Liquid Mixtures*, ed. O. Madelung, Volume 6., 1991, pp. 5–69.

16 G. Horwitz, M. Factorovich, J. Rodriguez, D. Laria and H. R. Corti, *ACS Omega*, 2018, **3**, 11205–11215.

17 V. K. Singh, Shalu, L. Balo, H. Gupta, S. K. Singh and R. K. Singh, *J. Solid State Electrochem.*, 2017, **21**, 1713–1723.